CERIA COATED MICROCHANNEL REACTOR FOR WATER-GAS SHIFT REACTION

by

Begüm Koca

B.S., Chemical Engineering, Middle East Technical University, 2014

Submitted to the Institute for Graduate Studies in
Science and Engineering in partial fulfillment of
the requirements for the degree of
Master of Science

Graduate Program in Chemical Engineering Boğaziçi University

Boğaziçi University

2016

CERIA COATED MICROCHANNEL REACTOR FOR WATER-GAS SHIFT REACTION

APPROVED BY:

Prof. Ahmet Kerim Avcı ..... (Thesis Supervisor)

Prof. Ayşe Nilgün Akın .....

Prof. Ramazan Yıldırım .....

DATE OF APPROVAL: 29.06.2016

ACKNOWLEDGEMENTS

From very begining, it was a great opportunity for me to work with Prof. Ahmet Kerim Avcı. I would like to express my sincere thanks to my supervisor Prof. Ahmet Kerim Avcı, whose wisdom, encouragament and support became a guadience for me to find my way during my MS thesis. I feel very grateful for both meeting with him and having the opportunity to work with him. I am nearly sure that my thesis would not be possible without him.

I would like to acknowledge my thesis committee members, Prof. Ramazan Yıldırım and Prof. Ayşe Nilgün Akın for devoting their valuable time to read and comment on my thesis.

I also want to thank Bilgi Dedeoğlu, Murat Düzgünoğlu, Belgin Balkan, Melike Gürbüz and Yakup Bal for their everlasting help. Thanks to Bilge Gedik Uluocak for their help in XRD, SEM and EDX analyses conducted at Boğaziçi University Research and Development Center.

Heartfelt thanks goes to my roommate and mastermate Tugçe Ilksoy, who always hold me close and share the grey times of mine. Her endless moral support and frienship brings me to the success. I gain here a lifetime friend.

I would like to thank to KB 404 members; Amin Delparish, Hatice Merve Can, Özgür Yaşar Çağlar and my special thank goes to Sinan Koç for his guidance during my thesis work. Their existence in the lab was a great source of motivation to study.

The memories of Teras will be a part of me forever. I would like to thank all super Teras Night members, Pelinsu Bulutoğlu, Damla Uckan, Doğa Fındık and Suat Canberk Ozan. Although we are on crossroads now, here's where fun begins. Hopefully, we will meet again in the light of efes malt.

I would like to thank to my all friens in this department especially, Deniz Irvalı, Pınar Eribol and Buge Yılmazer for their support and friendship.

I thank to those whom contributed and will contribute to my existence, I wish I would have thousands of pages to explain every hardness of my life and the ways that I struggled to overcome them. Like Frank Sinatra stated, every one lives according to their own way and I did it my way. Let's finish with one of my favourites, The mind is everything. What you think you become.

I devote this thesis to my family, whose everlasting faith courge me to success and who were with me at every hardness. I would like thank to all them seperately. Thanks to my father and mom, Yücel Serhan Koca and Leman Koca, with their unconditional love and encouragement, every succes of mine became possible. To my sister and brother, Buke Oz and Barkın Serhan Koca, without their brotherly and sisterly love, I would be incomplete.

Financial support for this work is provided by TÜBİTAK (project no: 113M229) and by BAP (project no: 8460).

ABSTRACT

CERIA COATED MICROCHANNEL REACTOR FOR WATER-GAS SHIFT REACTION

In this study, it is aimed to develop a method for coating $Pt/CeO_2/Al_2O_3$ catalyst onto the FeCrAlY-based wall of a microchannel reactor and to study water-gas shift (WGS) in the context of a parametric study. Firstly, the development of catalyst coating method is examined. The biggest concern about coating was the instability of the coated layer, which came from the presence of CeO2. Therefore, it is decided to use polyvinyl alcohol (PVA) as a binder between the metal surface and the catalyst. After a number of trials including the optimization of the amount of PVA, drying and calcination programs and the way of coupling PVA and the catalyst, a procedure that allowed stable coating of the catalyst was developed. The second part of the study involved investigation of the effect of reaction temperature (300, 325 and 350 °C) and molar inlet steam-to-carbon ratio (S/C=2 and 3) on CO conversion in the catalyst coated microchannel reactor. It was observed that conversions notably increased with the temperature, but responded slightly upon changing S/C. The highest CO conversion of 12.96 was achieved at 350 °C and S/C=2. Additionally, the effect of different amounts of catalyst loadings on FeCrAlY plates was examined. The results revealed that 6 and 12 mg coatings do not show the same level of difference in terms of CO conversion. Interestingly, 9 mg catalyst coating gave conversions slightly lower than those of 6 and 12 mg coatings. Finally, the effect of the different microchannel reactor configurations, coated and packed microchannels, was explored under identical residence times, defined as the ratio of catalyst weight to the total volumetric inlet flow rate. It was observed that, in general, coated configuration gave slightly higher conversions than the packed one, possibly due to better heat distribution and catalyst utilization in the former.

ÖZET

SU-GAZI GEÇİŞİ REAKSİYONU İÇİN SERYUM OKSİT KAPLI MİKROKANAL REAKTÖRLER

Bu çalışmada %1.5 Pt/% 5 CeO_2/Al_2O_3 katalizörünün FeCrAlY temelli mikro kanal duvarına kaplanabilmesi için bir yöntem geliştirilmesi ve su-gazı geçiş reaksiyonunun parametrik bir çalışma kapsamında incelenmesi amaçlanmıştır. Çalışmada ilk olarak katalizör kaplama yöntemi araştırılmıştır. Kaplamalar ile ilgili en büyük sorun kaplanan yüzeyin CeO_2 varlığı nedeniyle kararlı olmamasıdır. Bu nedenle, polivinil alkolün (PVA) katalizör ve metal yüzey arasında yapıştırıcı katman olarak kullanılmasına karar verilmiştir. Bir dizi deneme çalışmasının sonunda, kullanılacak PVA miktarı, kurutma ve kalsinasyon yöntemleri ve PVA ve katalizörün temas ettirilme yöntemi gibi parametreler optimize edilerek kararlı kaplamaların yapılabilmesine imkan tanıyan bir yönteö geliştirilmiştir. Çalışmaların ikinci bölümünde, reaksiyon sıcaklığının (300, 325 ve 350 °C) ve besleme akımındaki molar su buharı/karbon (S/C=2 and 3) oranının kaplı mikrokanal reaktörde CO dönüşümü üzerine olan etkileri incelenmiştir. Deneyler süresince dönüşümlerin sıcaklığa bağlı olarak büyük ölçüde değiştiği, ancak besleme kompozisyonun değişimiyle daha az bir değişiklik gösterdiği gözlemlenmiştir. En yüksek CO dönüşümü olan 12.96, 350 °C ve S/C=2 koşullarında elde edilmiştir. Ek olarak, farklı miktarlarda katalizörlerin FeCrAlY plakalara kaplanmasının reaksiyon üzerindeki etkileri incelenmiştir. 6 ve 12 mg'lık kaplamaların sağladığı dönüşümlerin yakın oldukları gözlemlenirken, 9 mg'lık kaplamaların daha düşük dönüşümler verdiği tespit edilmiştir. Son olarak, reaktör düzeninin etkileri-kaplı ve dolgulu-, katalizör kütlesinin besleme akımındaki toplam hacimsel giriş hızına oranı olarak tanımlanan alıkonma süresinin denk olduğu koşullarda karşılaştırmalı olarak incelenmiştir.Deneyler sonucunda, kaplı mikrokanalların yüksek ısı transferi özellikleri sayesinde, dolgulu mikro kanallardan daha yüksek dönüşüm gerçekleştirdiği gözlemlenmiştir.

TABLE OF CONTENTS

ACKNOWLEDGEMENTS . . . iii
ABSTRACT . . . v
ÖZET . . . vi
LIST OF FIGURES . . . ix
LIST OF TABLES . . . xii
LIST OF SYMBOLS . . . xiv
LIST OF ACRONYMS/ABBREVIATIONS . . . xv
1. INTRODUCTION . . . 1
2. LITERATURE SURVEY . . . 4
2.1. Water-Gas Shift Reaction . . . 4
2.2. Microchannel Reactors . . . 6
2.3. Coating on Microchannel Reactors . . . 7
3. EXPERIMENTAL WORK . . . 9
3.1. Materials . . . 9
3.1.1. Chemicals . . . 9
3.1.2. Gases and Liquids . . . 9
3.2. Experimental Systems . . . 10
3.2.1. Catalyst Preparation Systems . . . 11
3.2.2. Catalyst Characterization System . . . 11
3.2.3. Catalytic Reaction System . . . 12
3.2.4. Product Analysis System . . . 14
3.3. Catalyst Preparation and Pretreatment . . . 15
3.3.1. Catalyst Preparation . . . 15
3.3.2. Catalyst Coating on Microchannel Plates . . . 16
3.3.3. SEM/EDX Analyses for different Catalyst Types . . . 17
3.4. Reaction Tests . . . 18
3.4.1. Blank Tests . . . 18
3.4.2. WGS in Coated Microchannel Reactor . . . 18
3.4.3. WGS in Packed Microchannel Reactor . . . 21

4. RESULTS AND DISCUSSIONS 23
4.1. Development of catalyst coating procedure 23
4.2. Effect of temperature on CO conversion 30
4.3. Effect of S/C ratio on CO conversion 31
4.4. Effect of coated catalyst loading on CO conversion 32
4.5. Effect of reactor configuration on CO conversion 37
5. CONCLUSIONS AND RECOMMENDATIONS 41
5.1. Conclusions 41
5.2. Recommendations 42
REFERENCES 43
APPENDIX A: MFC CALIBRATION CURVES 46
APPENDIX B: GC CALIBRATION CURVES 48

LIST OF FIGURES

Figure 3.1. The Impregnation System: 1. Ultrasonic Mixer, 2. Buchner Flask, 3. Vacuum Pump, 4. Peristaltic Pump, 5. Aqueous Catalyst Solution, 6. Silicon Tubing [1]. 12

Figure 3.2. Schematic Representation of the Reaction System. 1. Gas Regulators, 2. Mass Flow Controllers, 3. On-Off Valves, 4. Three-Way Valves, 5. Thermocouple Locations, 6. Mixing Zone, 7. Quartz Tube [1]. 13

Figure 3.3. Plate image after coating. 17

Figure 3.4. SEM images of Pt/CeO2/Al2O3 with and without PVA (magnification on the left panel images: 2500x , magnification on the right panel images: 5000x). 18

Figure 3.5. Coated Microchannel Reactor Configuration. a. Coated microchannel reactor b. Location of steel housing in quartz tube [1]. 19

Figure 3.6. Packed Microchannel Reactor Configuration. a. Channel and catalyst configuration b. Location of steel housing in quartztube [1]. . 21

Figure 4.1. CO conversion vs. reaction temperature at different feed compositions. 31

Figure 4.2. Equilibrium CO conversions as a function of temperature for different feed compositions. 31

Figure 4.3. CO conversion vs. S/C ratio at different temperatures. 32

Figure 4.4. CO conversion vs. catalyst loading at different combinations of reaction temperature and feed composition. 33

Figure 4.5. Coated plate thickness vs. Length from the plate enterance measurements as a function of catalyst loading. 36

Figure 4.6. (a) SEM image from the middle of the PVA and 6 mg 1.5 wt% Pt /5 wt% CeO_2/Al_2O_3 coated plate, (b) SEM image from the middle of the PVA and 9 mg 1.5 wt% Pt /5 wt% CeO_2/Al_2O_3 coated catalyst. 36

Figure 4.7. SEM image from the top of the PVA and 12 mg 1.5 wt% Pt /5 wt% CeO_2/Al_2O_3 coated plate. 37

Figure 4.8. CO conversion vs. reactor configuration at different reaction temperatures (S/C=2). 38

Figure 4.9. CO conversion vs. reactor configuration at different reaction temperatures (S/C=3). 38

Figure 4.10. CO conversion vs. time (T=325 °C, S/C=3). 39

Figure A.1. MFC Calibration Curve of H_2. 46

Figure A.2. MFC Calibration Curve of CO. 46

Figure A.3. MFC Calibration Curve of CO_2. 47

Figure A.4. MFC Calibration Curve of N_2. 47

Figure B.1. GC Calibration Curve of H_2. 48

Figure B.2. GC Calibration Curve of CO. 48

Figure B.3. GC Calibration Curve of CO_2. 49

Figure B.4. GC Calibration Curve of N_2. 49

LIST OF TABLES

Table 3.1. Chemicals used for catalyst preparation. 9

Table 3.2. Specifications and applications of the liquids used. 10

Table 3.3. Specifications and applications of the gases used. 10

Table 3.4. Gas analysis conditions for product gas stream [2]. 15

Table 3.5. EDX analysis results in the presence of PVA and without PVA. . 17

Table 3.6. Experimental plan for WGS carried out in coated microchannel configuration. 20

Table 3.7. Feed conditions for WGS reaction in the study. 21

Table 3.8. Experimental plan for WGS carried out in packed configuration. . 22

Table 4.1 Methods investigated for coating of $Pt/CeO_2/Al_2O_3$ catalyst onto the FeCrAlY plate.(*cont.*) 25

Table 4.2. CO conversions obtained as functions of reaction temperature and S/C ratio. 30

Table 4.3. Different reaction conditions and catalyst loadings for the reactions and the conversion results. 33

Table 4.4. Thickness measurements for 6 mg catalyst loading at different points along the plate. 34

Table 4.5. Thickness measurements for 9 mg catalyst loading at different points along the plate. 35

Table 4.6. Experimental Road Map and Conversion Results 40

LIST OF SYMBOLS

C_{CO}^{in}	CO concentration in feed
C_{CO}^{out}	CO concentration in outlet
H	Height of the microchannel (mm)
K_{eq}	Parameter set
L	Length of the microchannel (mm)
T	Temperature (°C)
W	Width of the microchannel (mm)
ΔG	Gibbs free energy of reaction (kJ/mol)
ΔH	Standard enthalpy of reaction (kJ/mol)

LIST OF ACRONYMS/ABBREVIATIONS

DI	Deionized
GC	Gas Chromatograph
HPLC	High Performance Liquid Chromatography
HTS	High Temperature Shift
ID	Inner Diameter
LTS	Low Temperature Shift
MFC	Mass Flow Controller
PEMFC	Proton Exchange Membrane Fuel Cell
POX	Partial Oxidation
S/C	Steam-to-Carbon Ratio
SEM	Scanning Electron Microscopy
S/V	Surface to Volume Ratio
TCD	Thermal Conductivity Detectors
W/F	Catalyst Weight to Feed Flow Rate
WGS	Water Gas Shift

1. INTRODUCTION

Energy demand rises in parallel with increasing population and growing industrial world. Increasing the energy efficiency and decreasing the level of dependency on fossil fuels are two main driving forces to enhance new energy technologies. Thus, role of renewable energy sources to overcome the imbalance between the energy supply and demand cannot be ignored. There are several alternative energy sources like wind, hydro and solar energy. However, their applications do not eliminate the dependency of crude oil in their current technology level. Another promising clean technology is using hydrogen to generate energy via fuel cells. It is expected that hydrogen utilized fuel cells can reduce the dependence on fossil fuels. One of the most clean and efficient power source is Hydrogen-fueled proton exchange membrane fuel cell (H2-PEMFC) which can be used as a portable device thanks to its high power density, low operating temperature and rapid start-up. The main problem associated with the use of PEMFC is the distribution and storage of hydrogen. In order to overcome these drawbacks, it is proposed to generate required hydrogen from hydrocarbon fuels such as natural gas, gasoline and methanol in an on-board fuel processor. Additionally, it is important to avoid rapid deactivation of the platinum anode catalyst in PEMFC since Pt electrocatalyst can easily become poisoned in the presence of only 10 ppm CO. Among various CO clean-up methods, water-gas shift (WGS) reaction seems to be the most efficient and economical one compared with pressure swing adsorption (PSA) and methanation for removing CO from hydrogen-rich gas in a fuel processor [3].

WGS is a reversible and slightly exothermic reaction involving gas phase reactants/products and a solid catalyst. Since it is an exothermic process, the reaction is thermodynamically favored at lower temperatures. However, in order to achieve high reaction rates, it is often necessary to operate at higher temperatures which are not favored thermodynamically. The reaction is an well-established industrial process in which water in the form of steam is mixed with carbon monoxide to obtain hydrogen and carbon dioxide, as shown in Equation 1.1:

$$CO + H_2 \longleftrightarrow CO_2 + H_2 \qquad \Delta H = -41.2kJ/mol, \qquad \Delta G = -28.6kJ/mol \quad (1.1)$$

WGS reactors are conventionally used in steam reforming process for increasing the hydrogen content of the effluent of steam reformer units. Considering the impact of temperature on thermodynamics, WGS is conventionally employed in two modes, namely at high and low temperatures, which involve the use of Fe-Cr based and Cu/ZnO-based catalysts, respectively. However, operating conditions of fuel processing mentioned above are different from those of industrial practice in the sense that the former involves oxygen in the reformate, preventing the use of well known Cu/ZnO based catalysts due to their pyrophoric properties. As a result, use of WGS in fuel processing applications requires non-pyrophoric catalysts such as precious metal based ones. Generally precious metal-based WGS catalysts are categorized as platinum and gold which are investigated specifically for use in fuel cell applications. It is observed that the precious metal-based catalysts (mainly Pt, Rh, Ru, Au, and Pd) that are deposited on partially reducible oxides such as ceria, zirconia, titania, iron oxides, and mixed oxides of ceria (e.g. ceria-zirconia) are quite active in the 250-400 °C range [4].

WGS is known as the bulkiest unit in a fuel processor. Therefore, reducing the size of WGS unit is expected to be beneficial in terms of ending up with a compact fuel processor. At this stage the use of microchannel reactors becomes promising as they are known to have inherent advantages over the conventional units. The beneficial features of the microchannel reactors are high heat and mass transport rates thanks to extremely high surface to volume ratios, high selectivity due to narrow residence time distribution, inherent safety due to reduced inventory of chemicals utilized, simplified process control for effective process/materials screening due to extremely short response times, and no strict limit in size reduction or expansion of plant components since any production capacity is achievable by means of parallel operation. Under these conditions, it is suitable to choose microchannel reactor for WGS reaction.

Ceria containing precious metal catalysts are known to demonstrate high WGS acitivities [4]. Therefore, coupling the use of ceria-containing catalysts with microchannel reactors seems to offer increased catalytic performance together with compactness. However, coating of ceria supported or promoted catalysts onto a surface is somewhat challenging as the stability of the resulting coating is known to be usually low especially when the surface is metallic in nature. This problem, which seems to be a barrier for the use of ceria in WGS catalysts, constitutes the starting point of this work which is aimed to study the coating of $Pt\ /CeO_2/Al_2O_3$ catalyst onto the metallic (FeCrAlY based) surface of a microchannel reactor. The first part of this study, involves the development of a procedure for obtaining stable coatings of Pt/CeO2/Al2O3 over FeCrAlY surface. Testing of the coated catalyst in a microchannel reactor constitutes the second part of this study in which the effects of feed composition, reaction temperature and mass of catalyst coating are explored. Finally, in order to understand the effect of reactor configuration on WGS performance, the coated microchannel configuration is compared with the so-called packed microchannel geometry in which particulate form of $Pt\ /CeO_2/Al_2O_3$ catalyst is packed into an empty microchannel. A brief survey of literature about WGS, catalysts and microchannel reactors is presented in Section 2. Methods for synthesizing the catalysts and description of the reaction/analysis system, microchannel reactor configurations and the operating conditions are given in Section 3. Outcomes of the experiments as well as their discussion are provided in Section 4. Section 5 summarizes the main conclusions and recommendations for future studies.

2. LITERATURE SURVEY

2.1. Water-Gas Shift Reaction

The WGS reaction basically serves two main purposes, which are to attain desired levels of H2/CO ratio (which is important for syngas demanding processes) and to reduce CO content in methane steam reforming (SMR), the primary method to produce H2 for fuel cells. The critical role of WGS is removing the CO products from fuel cell because the anode catalyst is irreversibly deactivated above 10 ppm of CO.

Pressure could not affect the reaction thanks to constant volume from reactants to products. Reaction is moderately exothermic and reversible and conversion is equilibrium controlled. The equilibrium constant is given in Equation 2.1 and from equation it can be concluded that the constant decreases with increasing temperature. Consequently, high conversions are favored at low temperatures. However, exothermic nature of the reaction makes the reaction kinetically favorable at high temperatures. To be able to accomplish high conversions, the intersection of both kinetically and thermodynamically favorable region of the reaction should be taken into account. Therefore, utilization of WGS reaction is achieved in two sequential step, where the reaction is occurred both high and low temperatures. In the first part, the operating temperature is between 350-450 °C, therefore, called high temperature shift (HTS), whereas in second part the reaction is taken place as low temperatures in range of 190 to 250 °C and called low temperature shift (LTS) [5].

$$K_{eq} = exp\left(\frac{4577.8}{T(K) - 4.33}\right) \tag{2.1}$$

LT-WGS and HT-WGS are the two main steps for industrial WGS reactions in order to maximize hydrogen production, minimize reactor volume and handle trade-off between kinetics and thermodynamics [6]. The first stage is known as the high-temperature water-gas shift (HT-WGS) and most of the carbon monoxide is converted,

which is performed industrially at temperatures between 350 and 450oC. Fe_2O_3 / Cr_2O_3 catalysts are applied industrially for HT-WGS which are robust but suffer from low activity. The second stage (low-temperature water-gas shift, LT-WGS) is performed between 200 and 300oC over copper-zinc oxide catalyst depending on the application and the CO concentration required for the product [7]. Reformer gas first come over HT-WGS reactor and then passes through the LT-WGS reactor in order to attain CO concentrations at the ppm level [8]. Thus, WGS is carried out in a series of adiabatic converters in industry [4].

Due to the inherent disadvantages with the existing commercial catalysts, several authors have explained the use of noble metals as catalysts. Some of the concerns related with the commercial catalysis are given by Wheeler and co-workers (2004). The commercial Fe-based catalysts are prone to coke formation in the presence of excess fuel from the reformer. [9]. Because of the kinetic limitations, the use of the commercial Cu-based catalysts will occupy more volume. Moreover, the Cu-based catalyst is pyrophoric in reduced state and gets deactivated in the presence of condensed water due to leaching of active component or formation of surface carbonates [9] . The catalysts should also be capable of faster response during startup and shutdown. Hilaire and co-workers (2001) found the ceria supported transition metals acting as catalysts for the water gas shift reaction. After his studies on noble metal catalysis, it is found that the Pt/CeO_2 catalysts are more active than Au/CeO_2 and Au/Fe_2O_3. Wheeler (2004) studied the possibility of the WGSR using noble metals and metals with Ceria in the temperature range of 300°C to 1000°C and found the activity of the metals in the order, Ni,Ru,Rh,Pt,Pd. Most of the recent studies have been directed in using any of the precious metals like Pt, Rh, Pd and Au deposited on Ceria, Zirconia, Alumina, Titania, Thoria or Magnesia supports. Scientists have identified $Pt/CeO_2/Al_2O_3$ as the best candidate concerning selectivity and activity especially for application in a single stage medium temperature reactor.

2.2. Microchannel Reactors

Micro technologies and micro equipment gain more importance in last two decades, and become objects of great interest in chemical engineering. Research in the field of microscale devices has accelerated during the past 10-15 years [10].The possibilities offered by miniaturization of equipment take great attention due to ambition of achieving a fundamental change in design philosophy for chemical plants [3]. Extremely high surface to volume ratio (S/V) is achieved thanks to characteristic dimensions in microscale devices especially in microchannel reactors and they provide high surface area-to-volume ratios in the range of 10000 - 50000 m2/m3, while those of traditional reactors are generally about 100 m2/m3 and in rare cases reach 1000 m2/m3 [11]. Increased transfer area provides the advantage of transferring large amounts of energy between interfaces. Therefore, isothermal conditions can easily be achieved. In addition, due to high and efficient heat transfer rates, development of hot-spot formation or accumulation of reaction heat within microchannel reactors is prevented, and undesired side reactions are therefore suppressed [11]. Other several advantages over conventional-size reactors are

(i) Higher transport (e.g. heat and mass transfer) rates,
(ii) Safe environment for hazardous or toxic chemicals (due to low amount of chemicals used during process),
(iii) Simplify process control for effective process/materials screening (due to extremely short response time),
(iv) On-demand or on-site synthesis of critical chemicals such as H2O2, ethylene oxide,
(v) No strict limit in size reduction or expansion of plant components since any production capacity is achievable by means of parallel operation,
(vi) Development of integrated chemical analytical platforms as in microtonal analysis systems.

For chemical technologies, the applications of miniaturized reactions systems, or micro reactors, is centered on gas and liquid phase reactions covering simple mi-

croscale mixing of different fluids to volumetric titrations, heterogeneous and homogeneous catalysis, catalytic oxidation, heterocyclic synthesis, photochemical reactions and micro fuel cell applications. Due to higher yields and selectivities, the applications of environmentally more favorable reactions routes, and the possibility to replace large plants for distributed production according to actual demand, it is to be expected that micro technologies will eventually contribute to their sustainable development .

Not only heat transfer but also mass transfer demonstrate significant improvement in microchannel reactors compared to conventional reactors in terms of mixing times and short diffusion times. Mixing times decrease to several miliseconds and small channel dimensions provide short diffusion times; therefore, impact of mass transfer is observed as reduced reaction speed [11]. Additionally Sherwood number, which is described as mass transfer coefficient multiplied by hydraulic diameter divided by the diffusion coefficient, approaches a constant value in the developed laminar flow of a microchannel [12]. As a result, as the hydraulic diameter of the microchannel decreases, the mass transfer coefficient increases, which eliminate the mass transfer limitation [6].

High transport rates can be observed because transport rates are inversely proportional to channel diameters [11]. Moreover, due to small diameter nature, the radial diffusion time results in a narrow residence time distribution, which provides high selectivity to the desired intermediate for continuous processes [13]. Finally, less equipment and catalyst cost can be achieved thanks to inherent compact and portable nature of micro channel reactors.

2.3. Coating on Microchannel Reactors

The most common way to deposit catalysts within the microchannel is the wash-coating (slurry) technique. By this method catalyst that can be used directly and it is the biggest advantage of wash-coating method. On the other hand while depositing catalyst within a micro channel catalyst immobilization into microchannel can be occurred ant it can cause a low interaction between substrate surfaces and catalyst. Most research studies use inorganic binder to improve adherence. For commercial

$CuO/ZnO/Al_2O_3$ catalyst, alumina sol was often used as a binder [14]. Some researchers also used ZrO2 sol as binder to immobilize the catalyst onto a stainless steel microchannel. Nevertheless, using inorganic binder has some disadvantages. Chen (2011) reported that catalytic activity was significantly affected by the acidic sol because the catalysts were partially dissolved in the acidic slurry. It is also determined that the low pH of the catalyst slurry caused catalyst dissolving. Lin (2011) also reported that catalyst activity decreases as the ratio of CeO_2 sol increases in the catalyst slurry. Thus, inorganic binder is not recommended because the catalyst's active regions may be covered by the inorganic sol [15].

Another strategy to enhance the adhesive strength is to use a pretreatment technique on substrate. Chemical treatment, such as sol-gel technique, which is mainly "Formation of an oxide network through polycondensation reactions of a molecular precursor in a liquid". A sol is a stable dispersion of colloidal particles or polymers in a solvent. A gel consists of a three dimensional continuous network, which encloses a liquid phase. In a colloidal gel, the network is built from agglomeration of colloidal particles. In a polymer gel the particles have a polymeric sub-structure made by aggregates of sub-colloidal particles. In most gel systems used for materials synthesis, the interactions are of a covalent nature and the gel process is irreversible. Compared to traditional catalyst support, such as porous ceramic material, coating a silicon substrate with a catalyst faces more challenges [15]. Thus,it is suggested that the best way to achieve a good adhesive coating on a micro channel reactor is to use of PVA (poly vinyl alcohol) with the sol-gel method.

3. EXPERIMENTAL WORK

3.1. Materials

3.1.1. Chemicals

All chemicals used for catalyst preparation are presented in Table 3.1.

Table 3.1. Chemicals used for catalyst preparation.

Chemicals	**Formula**	**Source**	**Molecular Weight (g/mol)**
Gamma alumina	$\gamma - Al_2O_3$	Alfa Aesar	101.96
Poly(vinylAlcohol)	$[-CH_2CHOH-]_n$	Sigma-Aldrich	85-124.000
Cerium(III) nitrate hexahydrate	$Ce(NO_3)_3.6H_2O$	Sigma-Aldrich	434.22
Tetraammineplatinum(II) nitrate	$Pt(NH_3)_4(NO_3)_2$	Sigma-Aldrich	387.22

3.1.2. Gases and Liquids

The supplier for the all gases used in experimental setup was Linde Group, Istanbul. Zeneer Water Purification System provided the deionized water, which is used as liquid reactant and also used in catalysis synthesis, and its conductivity is less than 0.1 μS.cm-1. All liquids and gases used in the experimental study are presented in Table 3.2 and Table 3.3 respectively.

Table 3.2. Specifications and applications of the liquids used.

Liquid	**Specification**	**Application**
Water	Deionized(DI)	Catalyst Synthesis,Reactant

Table 3.3. Specifications and applications of the gases used.

Gas	**Specification(%)**	**Application**
Argon	99.995	GC Carrier Gas
Helium	99.999	GC Carrier Gas
Carbon monoxide	99.999	Product
Hydrogen	99.995	Product, Reducing Agent
Nitrogen	99.998	Inert

3.2. Experimental Systems

The experimental system used in this study is composed of four sub-systems:

- Catalyst Preparation Systems: These systems include furnaces for support preparation and incipient-to-wetness impregnation set-up for catalyst preparation.

- Catalyst Characterization System: In order to make qualitative and quantitative analysis of the catalyst samples and to measure the thickness of the coated catalysts, Scanning Electron Microscopy (SEM) integrated with Energy Dispersive X-ray Spectroscopy (EDX), which are present in Bogazici University Advanced Technologies R&D center, is used.

- Catalytic Reaction System: The system composed of a feed section including mass flow controllers for inlet gases, HPLC pump for water feed and a furnace for temperature control of the microchannel reactor.

- Product Analysis System: This system involves two online gas chromatographs which are used to carry out qualitative and quantitative analysis of feed and product mixtures.

3.2.1. Catalyst Preparation Systems

Sequential impregnation technique is used to prepare the 1.5%Pt/5%CeO2/Al2O3 catalysts. Buchner flask, vacuum pump (for pore opening), Retsch UR1 ultrasonic mixer (for uniform mixing) and Masterflex peristaltic pump (for impregnation of active metal solution onto the support) are the main units of the catalyst preparation system. Schematic representation of the entire system is shown in Figure 3.1. The first step in catalyst preparation is to evacuate the support at 105 °C in a vacuum furnace. The evacuated support is then put inside a Buchner flask which is then immersed into the Retsch UR1 ultrasonic mixer that provides constant vibration for 30 minutes under vacuum conditions with the help of a vacuum pump. By the help of adding the calculated amount of tetraamineplatinum(II) nitrate into 1.7 ml of deionized water, the active metal solution is prepared. The final solution is mixed till homogeneous mixture is achieved. Impregnation of the resulting solution to the support procedure is started by using a Masterflex peristaltic pump at a flow rate of 0.5 ml/min. Making sure that the solution is spread equally over the support material, the catalyst slurry is left over the ultrasonic pump for 90 minutes to achieve uniform dispersion. As a final step, drying and the calcination procedure is applied. For drying, the slurry left in a furnace at 115°C for 16 hours to remove water coming from impregnation. Finally, the dried catalyst is calcined at 300°C for 3 hours.

3.2.2. Catalyst Characterization System

Characterization of the catalyst samples and measurement of the thickness of the coated catalysts were carried out at Bogazici University Advanced Technologies R&D Center through Scanning Electron Microscopy (SEM) and Energy Dispersive X-ray Analysis (EDX) using a Philips XL30 ESEM-FEG unit.

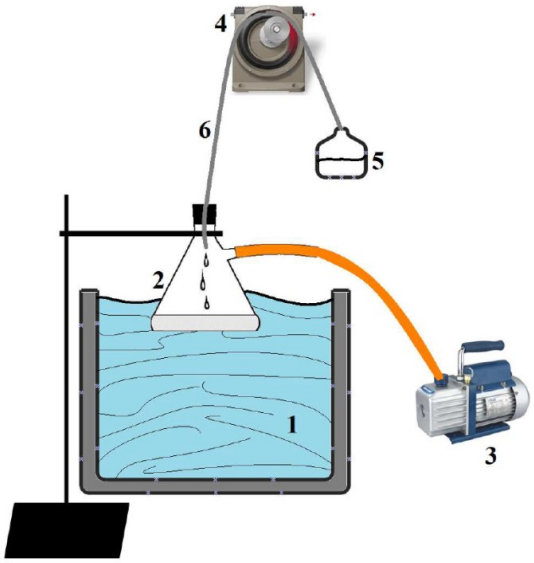

Figure 3.1. The Impregnation System: 1. Ultrasonic Mixer, 2. Buchner Flask, 3. Vacuum Pump, 4. Peristaltic Pump, 5. Aqueous Catalyst Solution, 6. Silicon Tubing [1].

3.2.3. Catalytic Reaction System

The catalytic reaction system, shown in Figure 3.2, is composed of feed and reaction sections. Pressurized gas cylinders, Shimadzu LC-20AD HPLC pump and Bronkhorst model F-201CV digital mass flow controllers (MFC) are the main parts of feed section. Reactant gas CO and inert N2 are stored in pressurized cylinders whose pressures can be controlled by two-stage regulators. After regulators, gas flows are sent to corresponding MFCs independently through 1/8" tubings. Flow rate of the gases are determined from calibration curves of MFCs provided in Appendix A. The resulting gas mixture is either directed to the reaction chamber or to gas chromatographs for feed analysis by means of a three-way valve.

Feeding of deionized water, which is used as liquid reactant, is done by a Shimadzu LC-20AD HPLC pump. For the transportation of liquid reactant to the system, 1/16" stainless steels tubing from Swagelok is used. It is necessary to vaporize liquid and keep it at 120 °C because it has to merge into the reactor feed at same conditions with

the feed gases. The control over the temperature of the liquid flow tubing is provided by heating tapes and integrated K-type thermocouples that provide feedback to digital on-off temperature controllers. Just before the entrance of the reactor, another three-way valve is used to divert the flow towards ventilation for 30 min., which is required for steady and well-mixed reactants flow before the mixture reaches the catalyst.

The reaction unit is composed of a 1.0 cm ID x 80 cm quartz reactor which is located in a vertical tubular furnace. Temperature control of the furnace is implemented by a Shimaden FP23 Programmable Temperature Controller and a K-type sheathed thermocouple. The position of the housing, which has the catalytic microchannel inside, is arranged to be in the constant temperature zone of the furnace for preventing temperature fluctuations through the thermocouple measurements. The reactor exit stream is either directed to ventilation through a soap bubble meter (for flow measurements) or sent to cold traps in series, where Dewar flasks are used to sustain the temperature of the cold traps for separation of unreacted water from rest of the gases. Effluent of the second cold trap is then directed to the gas chromatograph (GC) units via a three-way valve (Figure 3.2). Details of the gas chromatographs used in this study are given in Section 3.2.4.

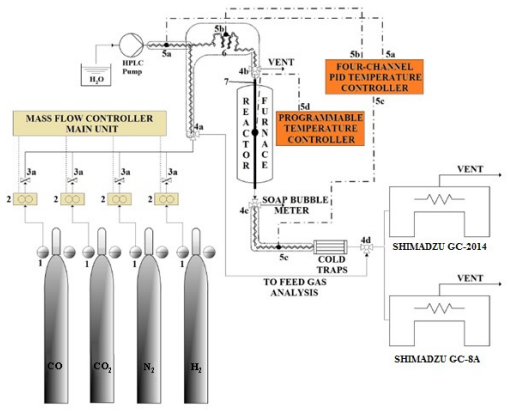

Figure 3.2. Schematic Representation of the Reaction System. 1. Gas Regulators, 2. Mass Flow Controllers, 3. On-Off Valves, 4. Three-Way Valves, 5. Thermocouple Locations, 6. Mixing Zone, 7. Quartz Tube [1].

3.2.4. Product Analysis System

Product analysis is performed on dry basis and carried out in two different GCs. Shimadzu GC-2014 has a Carboxen 1000 packed column, which can detect a H_2, N_2, CO, CH_4 and CO_2. The second GC, Shimadzu GC-8A contains a Porapak-Q column which can detects only N2, CO_2 and CH_4 (if present). Both of the GCs are equipped with thermal conductivity detectors. Operating parameters of GC units are summarized in Table 3.4.

Table 3.4. Gas analysis conditions for product gas stream [2].

	GC-2014	**GC 8A**
Carrier gas	Argon	Helium
Carrier gas flow rate	30 ml.min-1	25 ml.min-1
Column Temperature	40°C (0→13.5 min) 40 →150 °C 150 °C (15.5→27.5 min)	90 °C (12 min)
Column tubing material	Stainless steel	Stainless steel
Column packing material	Carboxen 1000	Porapak Q
Detector current	50 μA	120 μA
Detector type	TCD	TCD
Detector temperature	175 °C	150 °C
Injector temperature	110 °C	90 °C
Sample loop volume	1 ml	1 ml
Gases analyzed	H_2, N_2, CO_2, CO	N_2, CO

The first analysis is done in Shimadzu GC-8A with the outlet stream of the cold trap. Thereafter, the three-way valve is immediately turned to the Shimadzu GC-2014 for two minutes. Both GC units are equipped with manual gas sampling valves, each of which contain a sample loop with a volume of 1 ml.

During sampling, the sampling valve is kept at discharge position for 15 seconds to make sure that the gas sample is completely injected to the GC.

While performing the experiments, compositions and the amounts of the gas feedings is calculated according to the calibrations of both gas chromatographs and the mass flow controllers. Identity and the quantity of the gas are determined from retention times and areas under the curves of the GC, that means each gas forms a unique peak at a specific retention time. The area of a peak is the indicator of how much of that species (in terms of volume) is present in a 1 ml of sample. The calibration curve for each gas is constructed as area versus percentage accordingly and is presented in Appendix B.

3.3. Catalyst Preparation and Pretreatment

3.3.1. Catalyst Preparation

Sequential impregnation technique is used for the preparation of 1.5 wt% Pt /5 wt% CeO_2/Al_2O_3 catalyst [16]. 3 micron size of γ-Al_2O_3 is used as the support material. Firstly the drying procedure is applied in a vacuum furnace to evacuate the pores of the support. After drying at 150 °C for 1 hour, the support is positioned in a Buchner flask inside Retsch UR1 ultrasonic mixer for 30 min. The metal solution, which contains 0.135 gr of cerium (III) nitrate hexahydrate and 1.8 ml of deionized per gram of support, is fed to the Buchner flask with a flow rate of 0.5 ml/min via Masterflex peristaltic pump. After mixing the resulting slurry for 90 min under vacuum condition, the slurry is first dried for 16 hours at 115 °C in a furnace and then it is calcined for 3 hours at 300 °C in a muffle furnace. Afterwards, cooled ceria impregnated alumina is placed inside a Buchner flask, and same procedure with the ceria impregnation is applied to achieve the tetraamineplatinum (II) nitrate impregnation. The metal solution, which includes 0.053 gr of tetraamineplatinum (II) nitrate is added to 1.8 ml of deionized water per gram of slurry, is mixed and impregnated to the previously prepared slurry via a Masterflex peristaltic pump with a flow rate of 0.5 ml/min. The platinum impregnated ceria alumina is mixed for 90 min and is dried for 16 hours at

115 °C in a furnace. It is crushed and the calcined for 3 hours at 300 °C in a muffle furnace. The final form of catalyst is stored in a desiccator for further utilization.

3.3.2. Catalyst Coating on Microchannel Plates

The microchannel reactor is comprised of 310-grade stainless steel single channel cylindrical housing with diameter of 18.6 mm and length of 30 mm and FeCrAlY plates with dimensions of 2 mm x 5 mm x 20 mm, which are inserted into stainless steel housing. In order to prepare the plates for the coating, calcination is needed as a pre-treatment for FeCrAlY plates. Calcination is done at 900 °C for 3 hours in a muffle furnace, which ensures the formation of a native alumina layer on the plates. Thanks to alumina layer, the adhesion of the catalyst coating increases considerably [17].

The coating procedure for 1.5 wt% Pt/5 wt% CeO_2/Al_2O_3 catalyst on micro channel surfaces is difficult due to low adhesion tendency of ceria [18]. In order to achieve stable coating on the FeCrAlY surface, polyvinyl alcohol is utilized. As a first step, 2.93 gr polyvinyl alcohol (PVA) is dissolved in 50 ml deionized water at 85 °C for 2 hours by continuous stirring with mechanical stirrer in a water bath. Then the solution is cooled down to the room temperature. Cooled solution is applied to the steel surface and the prepared catalyst in powder form (Section 3.3.1) is applied directly on top of the PVA solution (Neuberg et al., 2014). Coated amount of catalyst is in the range of 10-15 mg; above 15 mg coated catalyst starts to fall. PVA is used as an adhesive layer between the microchannel and catalyst surface. The most important point in coating is that catalyst should be immediately adsorbed in PVA layer to ensure stable attachment between the catalyst and the plate. Right after finishing the coating, the calcination procedure should be applied to the coated plate to avoid evaporation in PVA layer. Calcination is done in Nabertherm furnace at 300 °C for 12 hours. At the beginning the furnace temperature was 25 °C then in 12 hours period it heated up to 300 °C with the ramp rate of 0.5 °C/min. As a final step, the plates are inserted into the previously cleaned and dried housing. In order to manage a steady placement of the plate in the housing, certain amount of ceramic wool is inserted at the bottom of the housing. At the end of the preparation, single rectangular microchannel with

dimensions 0.75 mm (H) x 4 mm (W) x 20 mm (L) is obtained [19]. An image of the catalyst coated plate is shown in Figure 3.3.



Figure 3.3. Plate image after coating.

3.3.3. SEM/EDX Analyses for different Catalyst Types

As explained in Section 3.3.2, coating method includes the usage of PVA. In order to investigate possible effects of PVA on catalyst structure, Pt/CeO2/Al2O3 and Pt/CeO_2/Al_2O_3 with PVA catalysts are calcinated and reduced at the same conditions. For both catalysts, EDX and SEM test are carried out and the findings are given in Table 3.5 and Figure 3.4, respectively.

Table 3.5. EDX analysis results in the presence of PVA and without PVA.

	Calcinated Pt/CeO2/Al2O3 Wihtout PVA			**Calcinated Pt/CeO2/Al2O3 With PVA**			
	Weight Percent (%)			Weight Percent (%)			
Elements	1	2	3	1	2	3	4
O	28.58	26.06	26.36	29.13	29.06	29.49	29.39
Al	63.84	66.36	63.52	63.53	61.97	62.18	59.86
Pt	1.31	1.48	1.59	2.87	2.76	2.94	2.77
Ce	6.28	6.1	8.52	4.47	4.36	5.39	5.19

After the analyses, it is determined that the Pt and Ce elements show homogeneous distribution all over the plate. In general, actual amounts of Pt and Ce are close to their target values of 1.5% and 5%, respectively. Even though the Pt amount in

the presence of PVA is slightly higher than 1.5 %, this is believed to be due to the minor errors occured during the preparation of the active metal salt solution used in impregnation. In other words, PVA does not affect the amount of Pt and its dispersion to the catalyst surface. Moreover, PVA does not exist in the catalyst structure as its elements are not detected during EDX analysis.

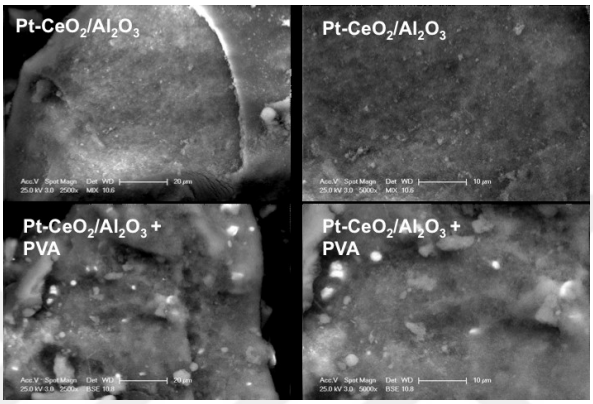

Figure 3.4. SEM images of Pt/CeO2/Al2O3 with and without PVA (magnification on the left panel images: 2500x , magnification on the right panel images: 5000x).

3.4. Reaction Tests

3.4.1. Blank Tests

Blank tests are performed under the reaction conditions (Section 3.4.2) to ensure that the materials of construction (i.e. quartz reactor tube, stainless steel housing, FeCrAlY plate), glasswool and alumina support have no catalytic activity. The results showed that these items remain inactive under the reaction conditions, as no CO conversion is detected.

3.4.2. WGS in Coated Microchannel Reactor

In coated microchannel configuration the experiments are conducted by using a quartz tube with an inner diameter of 20 mm, a 310-grade stainless steel housing and a catalyst coated FeCrAlY plate (Section 3.3.2, Figure 3.3). Stainless steel housing

(diameter=18.6 mm, length (L)=30 mm), shown in Figure 3.5a, is manufactured by electro discharge machining technique such that one coated FeCrAlY plate, with dimensions of 2 mm x 5 mm x 20 mm, can be inserted into it. Upon insertion, the remaining gap in the housing (Figure 3.5a) is defined as the coated microchannel with height (H), width (W) and depth of 0.75, 4 and 20 mm, respectively. As shown in Figure 3.3, the coatings on the sides of the plate, that overlap with the housing upon insertion, are removed to ensure smooth insertion of the plate to the housing. In order to make sure that the position of the plate remains unchanged in the housing, quartz wool is inserted into the last 10 mm gap between the plate and housing. Finally, housing with the coated plate is placed into the middle of the quartz tube and supported underneath by a hollow ring, which is demonstrated in Figure 3.5b. The hollow ring is an integral part of the quartz tube, which is then located within the furnace. As explained in Section 3.2.3, temperature of the reaction is measured by a K-type thermocouple, which is wrapped around the quartz tube, and controlled by a Shimaden FP23 PID temperature controller.

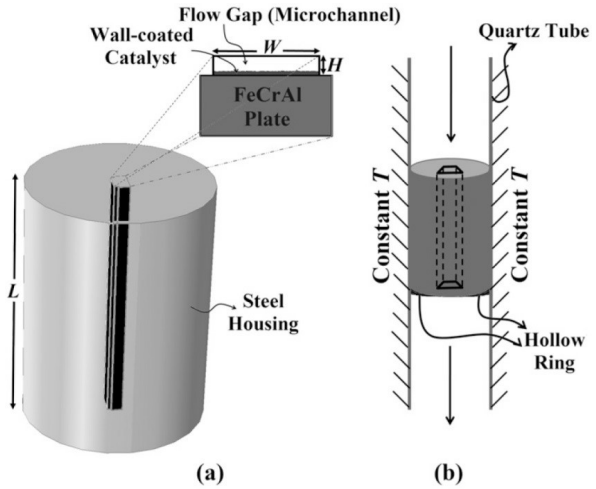

Figure 3.5. Coated Microchannel Reactor Configuration. a. Coated microchannel reactor b. Location of steel housing in quartz tube [1].

Plan of the experiments carried out in coated microchannel configuration is given in Table 3.6. During the experiments, it is aimed to investigate the effects of reaction temperature, molar inlet ratio of steam-to-carbon (S/C) and the mass of coated catalyst

on CO conversion, which is defined as the ratio of number of moles of CO converted to the number of moles of CO fed:

$$CO \quad Conversion(\%) = \frac{F_{CO}^{in} - F_{CO}^{out}}{F_{CO}^{in}} * 100 \tag{3.1}$$

The total flow rate in each experiment is kept constant at 80 Nml/min. Flow rates of the reactants that are arranged to obtain S/C ratio of 2 and 3 are given in Table 3.7. Prior to each experiment, the coated catalyst is reduced under pure H_2 flow 50 Nml/min at 300 °C for 3 h. Conversions are calculated from the outcomes of GC analyses which are carried out at the 30, 75, 120, 165 minutes from the beginning of the reaction. However, it is worth noting that the 30 min data is excluded from the conversion calculations to make sure that the operation reaches to its steady state. Therefore, CO conversions reported in this study belong to the arithmetic average of the conversions calculated at 75, 120 and 165 minutes.

Table 3.6. Experimental plan for WGS carried out in coated microchannel configuration.

S/C	**Temperature (°C)**	**Mass of catalyst coating (mg)**
2	300	6, 9, 13
2	325	6, 9, 13
2	350	6, 9, 13
3	300	6, 9, 13
3	325	6, 9, 13
3	350	6, 9, 13

Table 3.7. Feed conditions for WGS reaction in the study.

Steam/Carbon	**CO (Nml/min)**	**H_2O (Nml/min)**	**N_2 (Nml/min)**	**Total Flow Rate (Nml/min)**
2	20	40	20	80
3	15	45	20	80

3.4.3. WGS in Packed Microchannel Reactor

The schematic representation of packed microchannel reactor system is shown in Figure 3.6. In this configuration particulate form of Pt/CeO2/Al2O3 catalyst is packed into an empty microchannel, which is generated by inserting a blank FeCrAlY plate to the housing (Figure 3.5). In order to prevent the loss of catalyst, glass wool is inserted to the bottom of the housing, i.e. to the 10 mm gap between the end of the plate and housing. As explained in Section 3.4.2 in detail, the housing including the packed microchannel is inserted into the constant temperature zone of the quartz tube, which is the placed into the furnace.

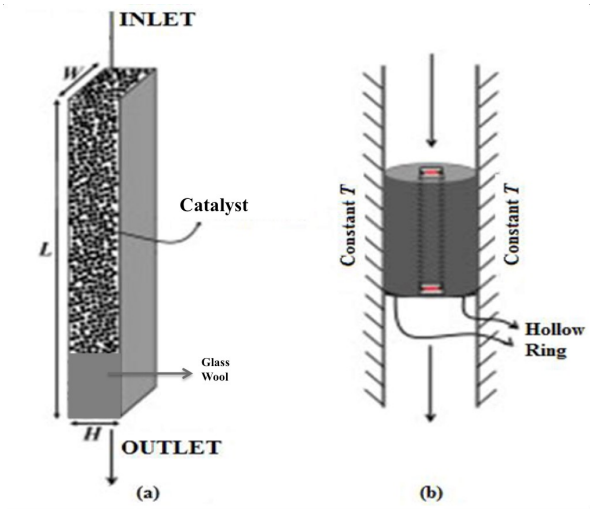

Figure 3.6. Packed Microchannel Reactor Configuration. a. Channel and catalyst configuration b. Location of steel housing in quartztube [1].

In packed microchannel configuration, the effect of reaction temperature and S/C are studied according to the plan given in Table 3.8. In the experiments, the mass of packed catalyst is kept constant at 13 mg. Outcomes of these experiments are compared with the ones carried out on coated microchannel configuration involving the same amount of coated catalyst.

Table 3.8. Experimental plan for WGS carried out in packed configuration.

S/C	**Temperature (°C)**	**Mass of packed catalyst (mg)**
2	300	13
	325	
	350	
3	300	13
	325	

4. RESULTS AND DISCUSSIONS

This section involves the results of WGS on ceria coated microchannel reactor and is divided into several sections. In the first section, coating results of $Pt/CeO_2/Al_2O_3$ is investigated for different amount of catalysts and the thickness test results are shown. The second section involves the results of SEM/EDX analyses for different catalyst loadings. In the third section, the effect of reactor configuration is investigated in the context of coated and packed microchannel reactor configurations.

4.1. Development of catalyst coating procedure

In order to obtain stable coating of the $Pt/CeO_2/Al_2O_3$ catalyst on the FeCrAlY plates, a number of methods are tested. Description of each method as well as the corresponding outcome is explained below. The methods together with the relevant quantitative details are summarized in Table 4.1. In order to prevent the loss of expensive Pt during the trials, part of the methods involved the use of CeO_2/Al_2O_3, which sufficiently describes the coating characteristics of the catalyst.

In the first method, PVA solution was mixed with CeO_2/Al_2O_3 sample in a beaker. Then the resulting suspension is applied to the FeCrAlY plate and after one day drying at 100 °C and 2 h of calcination at 300 °C, it was observed that the resulting coating have fallen from the FeCrAlY surface. In the second method, the conditions were the same with those of the first one except for the duration of drying which was 24 h at 100 °C. The resulting coating, however, turned out to be unstable. In the third method, the conditions were the same but the calcination is done immediately after 24 h drying at 100 °C. Calcination is carried out for 12 h and the ramp rate to reach 300 °C from room temperature was chosen as 1 °C/min. However, some burned parts in the coating were observed.. In the fourth sample another ramp rate, 0.5 °C/min, was used for calcination. Calcination started from 25°C and it took 12 h to reach 300 °C. At first this coating seemed to be stable, but after a while it again started to fall because of PVA, whose evaporation has led to the formation of bubble-like structures that

disturbed the stability of the coating. The explanation for this situation was that the PVA molecules could find the area for escaping because the suspension included both CeO_2/Al_2O_3 and the PVA solution, and there was no cover layer, like an additional catalyst surface, on top of the coating. In the fifth method, the amount of the PVA in PVA solution has reduced to 5 g PVA per 141 ml water, and it caused even a worse adhesive layer between the plate and the catalyst and some bubbles were observed at the coating. In the sixth method, the composition was reduced to 3 g PVA per 141 ml water. However, the required adhesion between coating and the FeCrAlY plate could not be obtained. A different coating procedure was tried in the context of seveth method. Instead of making a CeO_2/Al_2O_3 - PVA solution suspension, the PVA solution and CeO_2/Al_2O_3 were separately applied to the plates. First the PVA solution, which has 3 g PVA and 141 ml water, was applied. Then CeO_2/Al_2O_3 was added on top of the PVA layer. However the adhesive features of the solution was not strong because of the low PVA content. Thus the resulting coating turned out to be unstable. Only in the eighth sample a stable coating was obtained. The sequential application has performed together with using 8 g of PVA in the PVA solution, and the result turned out to be successful. With the help of the 141 ml water and 8 g PVA solution, 10 mg of 1.5 wt% Pt /5 wt% CeO_2/Al_2O_3 catalyst coating onto the FeCrAlY surface has been achieved. In order to increase the amount of coated catalyst on the plate, the ninth method that involved loading of 20 mg of catalyst was tried. However, it was observed that 20 mg was somewhat high for obtaining a stable coating. In other words, the amount of PVA solution required to bind 20 mg catalyst was insufficient. As a result, 10-13 mg of catalyst weight was determined as a limit for catalyst loading on a 5 mm x 20 mm heat treated FeCrAlY plate surface. Thus the eighth method was proven to be successful for obtaining a stable catalyst coating.

Table 4.1. Methods investigated for coating of $Pt/CeO_2/Al_2O_3$ catalyst onto the FeCrAlY plate.

Coating Method	**Observations & Results**
Method 1	
1. Preparation of PVA Solution: Mixing 141 ml water with 8 g PVA. 2. Coated Material: 5% CeO_2/Al_2O_3. 3. Coating Method: CeO_2/Al_2O_3 and PVA are mixed for 3 days, then mixture is put onto channel, immediately after 2 h drying, 2 h calcination is applied. 4. Drying Conditions: 100 °C, 2 h. 5. Calcination Conditions: 300 °C, 2h.	Coating has fallen significantly.
Method 2	
1. Preparation of PVA Solution: Mixing 141 ml water with 8 g PVA. 2. Coated Material: 5% CeO_2/Al_2O_3. 3. Coating Method: CeO_2/Al_2O_3 and PVA are mixed for 3 days, then mixture is put onto channel, immediately after 24 h drying, 2 h calcination is applied. 4. Drying Conditions: 100 °C, 24 h. 5. Calcination Conditions: 300 °C, 2 h.	Falling parts, which are less than method 1, are observed.
Method 3	
1. Preparation of PVA Solution: Mixing 141 ml water with 8 g PVA. 2. Coated Material: 5% CeO_2/Al_2O_3. 3. Coating Method: CeO_2/Al_2O_3 and PVA are mixed for 3 days, then mixture	It is determined that coating has some burned parts in the shape of little

Table 4.1. Methods investigated for coating of $Pt/CeO_2/Al_2O_3$ catalyst onto the FeCrAlY plate.(*cont.*)

Coating Method	**Observations & Results**
is put onto channel, immediately after 24 h drying, 12 h calcination with a rate of 1°C/min is applied. 4. Drying Conditions: 100 °C, 24 h. 5. Calcination Conditions: From 25 °C to 300 °C, with a rate of 1°C/min, calcined for 2 h at 300 °C.	black points. The reason for this situation could be the rapid heating of PVA.
Method 4	
1. Preparation of PVA Solution: Mixing 141 ml water with 8 g PVA. 2. Coated Material: 1.5% Pt/ 5 % CeO_2/Al_2O_3. 3. Coating Method: Catalyst and PVA are mixed for 3 days, then mixture is put onto channel, 12 h calcination with a rate of 0.5 °C/min is applied. 4. Drying Conditions: No drying. 5. Calcination Conditions: From 25 °C to 300 °C with a rate of 0.5 °C/min, calcined for 2 h at 300 °C.	The PVA and catalyst mixture segregate with time and the catalyst precipitate into the solution (this behavior does not observed in CeO_2/Al_2O_3 and PVA solution).Thus, it is concluded that PVA amount in sample was not sufficient and the coating was unsuccessful.

Table 4.1. Methods investigated for coating of $Pt/CeO_2/Al_2O_3$ catalyst onto the FeCrAlY plate.(*cont.*)

Coating Method	**Observations & Results**
Method 5	
1. Preparation of PVA Solution: Mixing 141 ml water with 5 g PVA. 2. Coated Material: 5 % CeO_2/Al_2O_3. 3. Coating Method: CeO_2/Al_2O_3 and PVA are mixed for 3 days, then mixture is put onto channel, 12 h calcination with a rate of 0.5°C/min is applied. 4. Drying Conditions: No drying. 5. Calcination Conditions: From 25 °C to 300 °C with a rate of 0.5 °C/min, calcined for 2 h at 300 °C.	Even if an homogenous solution has achieved, bubbles were observed on the coating.
Method 6	
1. Preparation of PVA Solution: Mixing 141 ml water with 3 g PVA. 2. Coated Material: 5% CeO_2/Al_2O_3. 3. Coating Method: CeO_2/Al_2O_3 and PVA are mixed for 3 days, then mixture is put onto channel, 12 h calcination with a rate of 0.5°C/min is applied. 4.Drying Conditions: No drying. 5.Calcination Conditions: From 25 °C to 300 °C with a rate of 0.5 °C/min, calcined for 2 h at 300 °C.	Coating has fallen as a layer because of the low concentration of PVA.

Table 4.1. Methods investigated for coating of $Pt/CeO_2/Al_2O_3$ catalyst onto the FeCrAlY plate.(*cont.*)

Coating Method	**Observations & Results**
Method 7	
1. Preparation of PVA Solution: Mixing 141 ml water with 3 g PVA. 2.Coated Material: 1.5% Pt/ 5 % CeO_2/Al_2O_3. 3.Coating Method : Firstly the PVA solution is applied to the channel,after that 10 mg catalyst is adsorbed into the solution, than from 25°C 12 hours calcination with 0.5°C/min rate is applied. 4.Drying Conditions: No drying. 5.Calcination Conditions: From 25 °C to 300 °C with a rate of 0.5 °C/min, calcined for 2 h at 300 °C.	Method 6 is applied for the reaction catalyst but the coating has fallen just because of the low concentration of PVA.
Method 8	
1. Preparation of PVA Solution: Mixing 141 ml water with 8 g PVA. 2.Coated Material: 1.5% Pt/ 5 % CeO_2/Al_2O_3. 3.Coating Method : Firstly the PVA solution is applied to the channel, after that 10 mg catalyst is adsorbed into the solution, than from 25°C 12 hours calcination with 0.5°C/min rate. 4.Drying Conditions: No drying. 5.Calcination Conditions: From 25 °C to 300 °C with a rate of 0.5 °C/min, calcined for 2 h at 300 °C.	After coating, a stable coating layer was achieved. The coating was successful.

Table 4.1. Methods investigated for coating of $Pt/CeO_2/Al_2O_3$ catalyst onto the FeCrAlY plate.(*cont.*)

Coating Method	**Observations & Results**
Method 9	
1. Preparation of PVA Solution: Mixing 141 ml water with 8 g PVA. 2.Coated Material: 1.5% Pt/ 5 % CeO_2/Al_2O_3. 3.Coating Method : Firstly the PVA solution is applied to the channel, after that 20 mg catalyst is adsorbed into the solution, than from 25°C 12 hours calcination with 0.5°C/min rate. 4.Drying Conditions: No drying. 5.Calcination Conditions: From 25 °C to 300 °C with a rate of 0.5 °C/min, calcined for 2 h at 300 °C.	The loaded amount of catalyst was in excess.Because of the excess amount, the some loses were observed.(nearly 7-8 mg of catalyst has fallen).

4.2. Effect of temperature on CO conversion

Outcomes of the effect of reaction temperature on CO conversion is reported in this section. Experiments are carried out on the coated microchannel configuration and the results are reported in terms of CO conversion in Table 4.2.

Table 4.2. CO conversions obtained as functions of reaction temperature and S/C ratio.

	Experimental Conversion (%)		**Equilibrium Conversion (%)**	
Temperature (°C)	S/C=2	S/C=3	S/C=2	S/C=3
300	3.49	5.11	97.5	98.7
325	4.87	4.74	96.6	98.3
350	12.96	8.88	95.5	97.4

Results have revealed that the temperature has a positive effect on CO conversion. However, experimental conversion (Table 4.2, Figure 4.1) and their equilibrium counterparts (Table 4.2, Figure 4.2) are significantly different from each other. Equilibrium conversions are calculated by using equation 2.1. The main reason for the low experimental conversions is due to the use of small catalyst quantities in the coated microchannel configuration. In other words, the residence time, defined as the ratio of mass of catalyst (W) to the total volumetric inlet flow rate (F) is ca. 5-10 times smaller than those involved in typical lab-scale packed bed reactors. As a result, the reactants contact with the catalyst in a very limited period of time, which limit the resulting conversions.

From the figures,it can also be noted that equilibrium conversions exhibit a decreasing trend with increasing temperature. This is expected as due to the Le Chatelier's principle that states negative effect of temperature on conversion in exothermic reactions.Since the experimental conversions increase with temperature it can be stated that the reaction kinetics dictate the overall process.

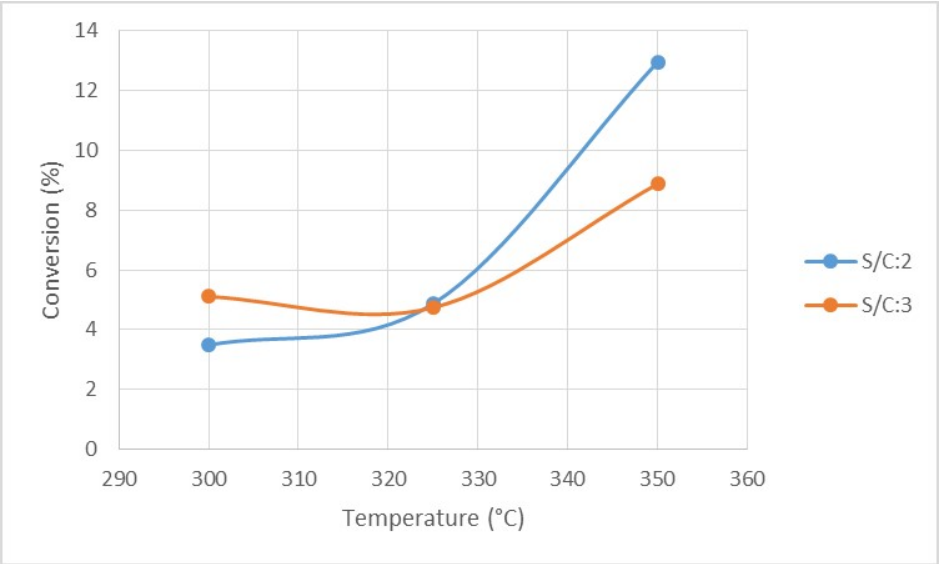

Figure 4.1. CO conversion vs. reaction temperature at different feed compositions.

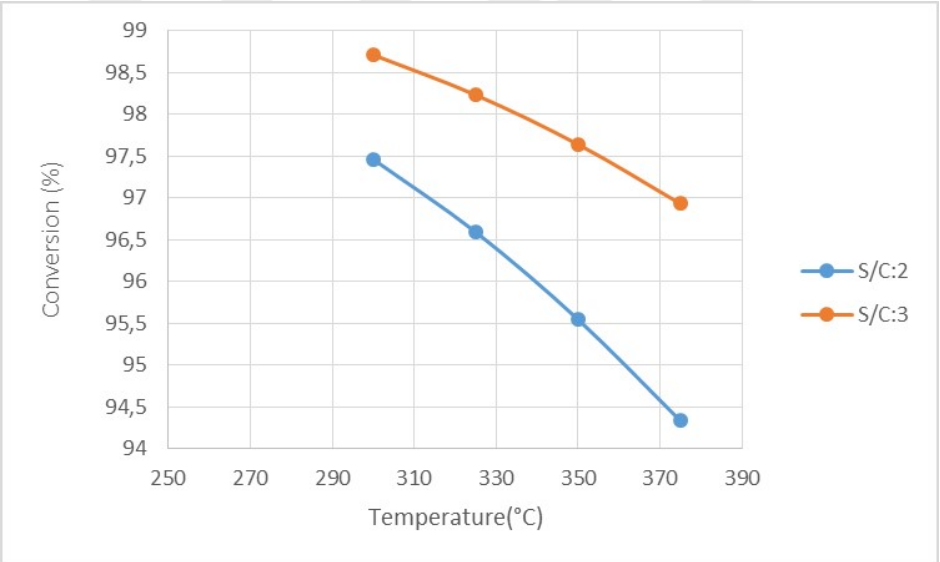

Figure 4.2. Equilibrium CO conversions as a function of temperature for different feed compositions.

4.3. Effect of S/C ratio on CO conversion

After reactions at different conditions it is determined that the S/C ratios has a slight impact on the conversion values. At 300 and 325 °C the conversion values

were found to be nearly the same for both S/C ratios. However, at 350 °C the conversion values have changed notably according to S/C ratios (Figure 4.3). In order to understand the possible reasons of the observed trends, a literature survey was done to examine the reaction kinetics for WGS reaction carried out over Pt-ceria catalysts. One of those studies showed that the rate directly proportional with the CO and steam amounts; partial pressure of CO affects the reaction rate in the order of 0.13, and the partial pressure of steam affects the rate in the order of 0.49 [20]. Thankfully, in this study, it is observed that, until 325 °C, the conversion values have verified the rate expression. However, above 325 °C, it is determined that the conversion values are higher when the S/C is 2. The conversion vs. temperature trend showed some unexpected changes especially at 350 °C. The possible reason for the situation could be changes in the reaction mechanism at higher temperatures. Some experimental errors or some misfortune in the experimental set up might also have caused this situation.

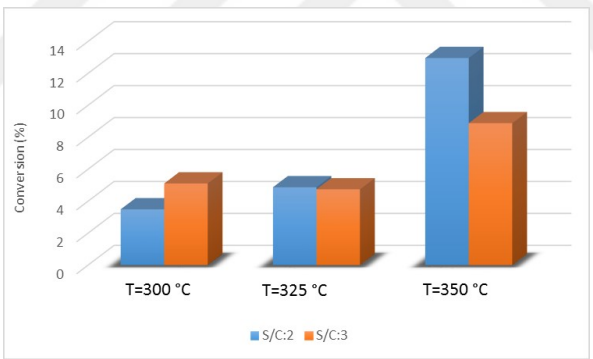

Figure 4.3. CO conversion vs. S/C ratio at different temperatures.

4.4. Effect of coated catalyst loading on CO conversion

In order to examine the effect of catalyst weight on CO conversion, different catalyst loadings are applied to the plates. Specified amounts for the coating are 6, 9 and 12 mg of catalyst. Experiments are performed for each catalyst loading and the results are listed in table 4.3. For a better comparison, the results are presented graphically in Figure 4.4.

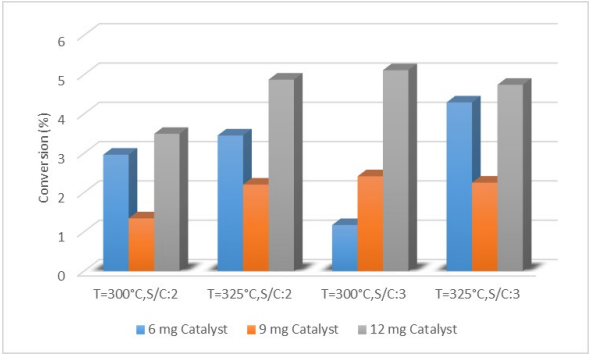

Figure 4.4. CO conversion vs. catalyst loading at different combinations of reaction temperature and feed composition.

Table 4.3. Different reaction conditions and catalyst loadings for the reactions and the conversion results.

S/C	**Temperature (°C)**	**Catalyst Weight (mg)**	**Conversion(%)**
2	300	6	2.96
2	300	9	1.34
2	300	12	3.49
2	325	6	3.45
2	325	9	2.2
2	325	12	4.87
3	300	6	1.17
3	300	9	2.41
3	300	12	5.11
3	325	6	4.29
3	325	9	2.11
3	325	12	4.74

As can be seen from Table 4.3 and Figure 4.4, the highest conversions belong to the 12 mg catalyst loading. After that, the conversions are higher in 6 mg catalyst loading rather than 9 mg catalyst loading. The reason for this situation could be the intra-layer diffusion limitations. When the catalyst is over loaded on to the plate, the

diffusion limitations might have become significant with increasing catalyst layer thickness. Thus the conversion observed in 9 mg catalyst loading could be lower than the conversion observed in 6 mg catalyst loading. On the other hand, 12 mg catalyst loading gives conversions that are slightly higher than obtained over 6 mg coated catalyst. The possible reason for this trend is due to counteracting effects of increased residence time and the intra-layer diffusion limitations. In other words, addition of extra 3 mg of catalyst might have reduced the diffusion limitation effect by causing an increase in residence time. In order to have an idea about the possibility of internal mass transfer resistance in the coated layers, thickness of the coated catalysts are measured by SEM technique and reported in Tables 4.4 and 4.5 for 6 and 9 mg catalyst coated plates, respectively. For each loading, thickness measurements are done at nine different points of the plate. For each point, the lowest and highest thickness values are measured and their average are reported.

Table 4.4. Thickness measurements for 6 mg catalyst loading at different points along the plate.

Measurement point from the entrance of the plate(mm)	**Average Thickness(μm)**
2	300
4	271
6	225
8	161
10	158
12	191
14	135
16	143
18	125

Table 4.5. Thickness measurements for 9 mg catalyst loading at different points along the plate.

Measurement point from the entrance of the plate(mm)	**Average Thickness(μm)**
2	612
4	395
6	313
8	316
10	420
12	274
14	337
16	340
18	301

The measurements reported in Tables 4.4 and 4.5 show that thicknesses change in accordance with the amount of catalyst. Thicknesses of 9 mg and 12 mg catalyst loadings (the latter is not reported) are similar and 6 mg catalyst loading is a little bit thinner than the 9 mg and 12 mg catalysts. The thickness comparison graph for 6 mg and 9 mg catalyst coated plate can also be seen in Figure 4.5. The SEM images of the thickness tests are presented in Figures 4.6 for 6 and 9 mg coatings, and in Figure 4.7 for 12 mg catalyst loadings, respectively.

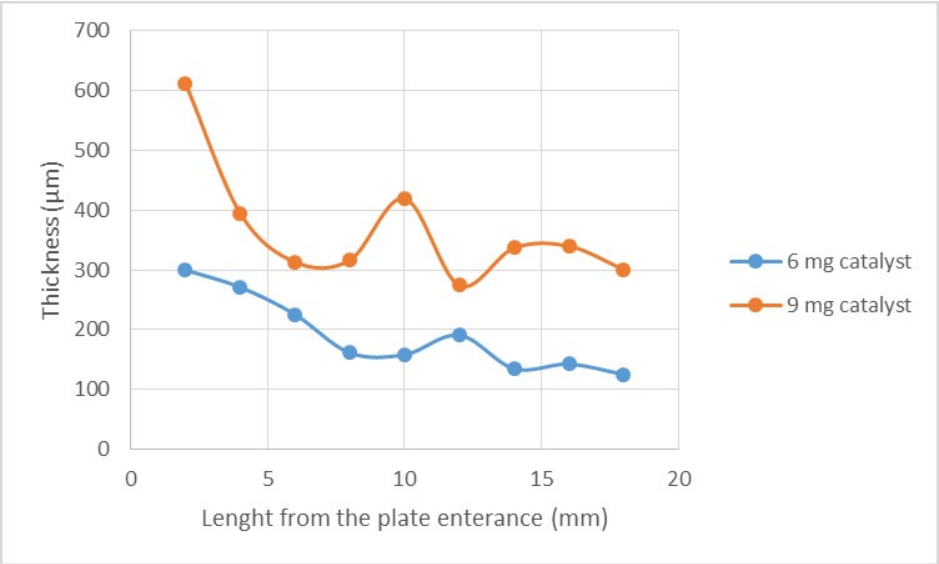

Figure 4.5. Coated plate thickness vs. Length from the plate enterance measurements as a function of catalyst loading.

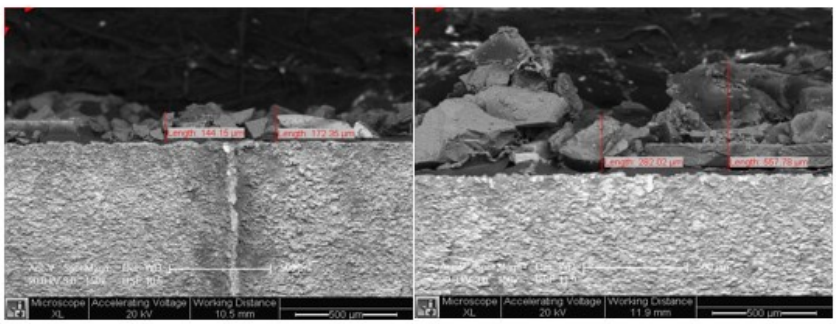

(a) (b)

Figure 4.6. (a) SEM image from the middle of the PVA and 6 mg 1.5 wt% Pt /5 wt% CeO_2/Al_2O_3 coated plate, (b) SEM image from the middle of the PVA and 9 mg 1.5 wt% Pt /5 wt% CeO_2/Al_2O_3 coated catalyst.

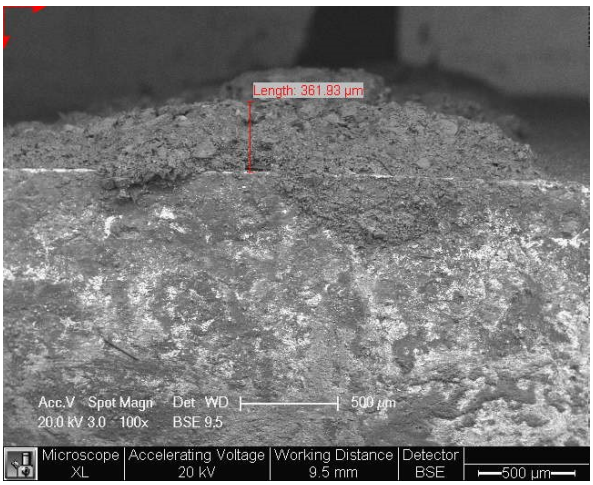

Figure 4.7. SEM image from the top of the PVA and 12 mg 1.5 wt% Pt /5 wt% CeO_2/Al_2O_3 coated plate.

4.5. Effect of reactor configuration on CO conversion

In order to understand the effect of reactor configuration, coated and packed microchannel reactors (see Sections 3.4.2 and 3.4.3, respectively) are comparatively studied at equal residence times defined as the ratio of catalyst weight to the total inlet volumetric flow rate. Outcomes of the comparisons are presented in Figures 4.8 and 4.9, and in Table 4.6. The results shows that, in general the conversions obtained in the coated microchannel are higher than those obtained in packed microchannel. The reason for this outcome is believed to be better heat transfer and effective catalyst usage features of the coated microchannel reactor. Coated microchannel reactors have some advantages over the packed ones [21]. In packed microchannel reactors, in addition to the slower rates of heat transfer due to the particular geometry of packed beds, high pressure drops and channeling of flow of reactants could be observed. However, in coated microchannel reactors, relatively lower pressure drop and higher heat and mass transfer characteristics are present. As the thin catalyst is coated on a thermally conductive metallic surface, transfer of external heat can be inherently fast.

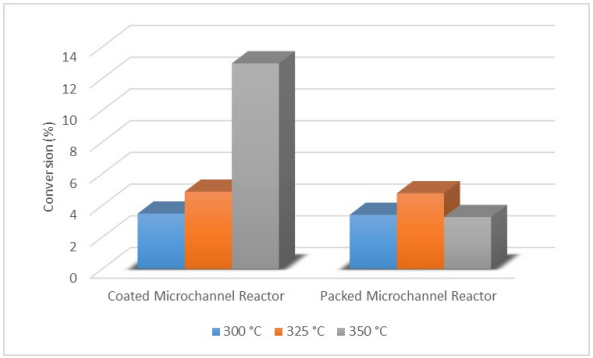

Figure 4.8. CO conversion vs. reactor configuration at different reaction temperatures (S/C=2).

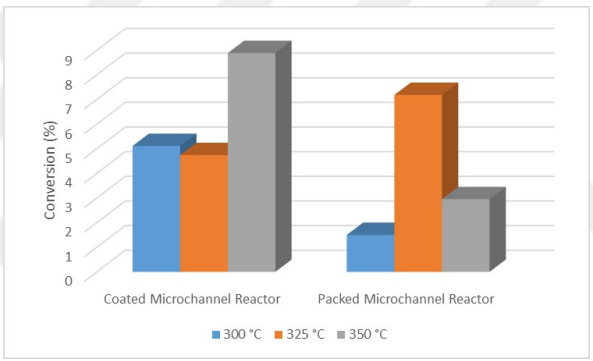

Figure 4.9. CO conversion vs. reactor configuration at different reaction temperatures (S/C=3).

Another interesting result is observed at 350 °C over packed microchannel configuration. The results shown in Figures 4.8 and 4.9 show that, upon increasing temperature from 325 to 350 °C conversion increases over the coated microchannel, whereas it decreases notable over the packed one. A possible reason of this outcome is the differences in the residence time distribution characteristics, which is inherently wider in the packed microchannel. In other words, in packed configuration, reactants can reside longer than expected, which allows the reverse WGS to become significant as a result of high temperature. On the other hand, distribution of residence time is narrower in the coated configuration, and the reactive stream can leave the catalyst bed before the reverse reaction becomes significant.

In order to verify the stability of the coating, a 24 h time-on-stream test is carried out in a 12 mg catalyst coated microchannel reactor. Temperature and the feed composition of the stability test were 325 °C and CO:H2O:N2=15:45:20, respectively. The sampling involved analysis of product mixture at every 45 min. The results shown in Figure 4.10 indicate a slow, monotonic decrease in CO conversion until 200 min, after which conversion remained almost unchanged. Moreover, the visual examination of the coated catalyst after the time-on-stream test showed that the coating remained stable, without any removal from the metallic surface. Based on these findings, it can be stated that the coating procedure explained in Section 4.1 turned out to deliver stable coating of the Pt/CeO2/Al2O3 catalyst.

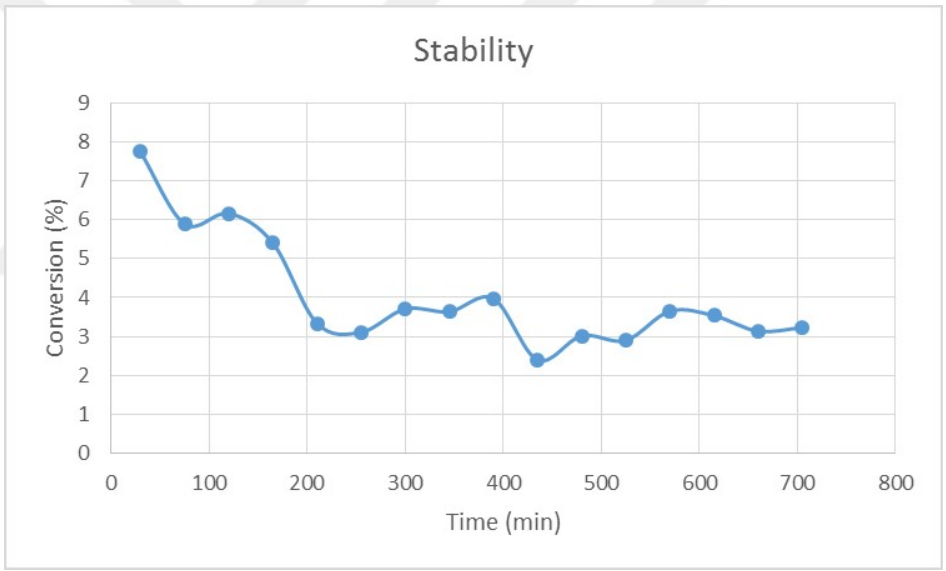

Figure 4.10. CO conversion vs. time (T=325 °C, S/C=3).

Table 4.6. Experimental Road Map and Conversion Results

Micro Reactor Configuration	**Flow Rates (Nml/min)**	**Catalyst Weight (mg)**	**Temperature (°C)**	**S/C**	**CO Conversion (%)**
Coated	CO: 20, H2O: 40, N2: 20	13	300	2	3.49
		13	325	2	4.87
		13	350	2	12.96
		13	375	2	6.99
		6	300	2	2.96
		6	325	2	3.45
		9	300	2	1.34
		9	325	2	2.20
	CO:15, H2O: 45, N2: 20	12	300	3	5.11
		12	325	3	4.74
		12	350	3	8.88
		6	300	3	1.17
		6	325	3	4.29
		9	300	3	2.41
		9	325	3	2.12
Packed	CO: 20, H2O: 40, N2: 20	13	300	2	3.41
		13	325	2	4.77
		13	350	2	3.27
	CO:15, H2O: 45, N2: 20	14	300	3	1.5
		13	325	3	7.18
		13	350	3	2.95

5. CONCLUSIONS AND RECOMMENDATIONS

5.1. Conclusions

The aim of this study is to develop a method for coating Pt/CeO2/Al2O3 catalyst onto the FeCrAlY-based wall of a microchannel reactor and to study water-gas shift (WGS) in the context of a parametric plan. The first phase of this study involved development of a procedure that allowed stable coating of the 1.5 wt% Pt /5 wt% CeO_2/Al_2O_3 catalyst to the surface of a FeCrAlY plate, which is an integral part of the microchannel reactor. The effects of reaction temperature, feed condition, catalyst loading and reactor configuration on CO conversion are studied in the second phase of this work. The main conclusions of this study can be summarized as follows:

- CO conversions increase with temperature. Highest conversion is found to be 12.96% at 350 °C with a feed composition CO:H2O:N2=20:40:20.

- It is found out that the presence of ceria makes the catalyst coating difficult on the FeCrAlY plates for microchannel reactor applications. By using PVA as a binder and after proper optimization of coating parameters (amount of PVA, duration and temperature of drying and calcination and the method of integrating PVA and catalyst), stable and reproducible coatings of Pt/CeO2/Al2O3 catalyst are obtained.

- Mass of catalyst coatings is limited to 13 mg on a 5 mm x 20 mm FeCrAlY surface. The limited catalyst amount also caused the resulting CO conversions to be less than ca. 13%.

- In SEM analysis, it is observed that porous structure of the catalyst is unaffected by the reduction and reaction conditions. Moreover, as also supported by EDX analysis, no coke formation and PVA contamination is detected on the catalyst structure.

- EDX analysis also reveals that the actual amounts of Pt and Ce in the resulting catalyst are close to their target values.

- The results revealed that, at 325 °C and above, CO conversions are higher when S/C=2. This trend changes at 300 °C where S/C=3 gives higher CO conversions. This change is believed to be due to a possible change in the behavior of the catalyst with temperature.

- Effect of mass of catalyst coating is investigated. The results showed that 6 and 12 mg catalyst loadings have nearly close conversion values but, 9 mg catalyst loading did not show as high conversions as in the 6 mg and 12 mg loading experiments.

- Effect of reactor configuration is also studied. It is observed that the coated configuration gave slightly higher conversions than the packed one.

5.2. Recommendations

Regarding the results of present work, following studies are recommended for future studies:

- The amount of CeO2 in the catalyst can be increased to observe its effect on the coating quality as well as on CO conversion. Similarly, the weight percent of Pt could be investigated as another parameter.

- As an alternative active metal, Au can be used in the future study. It is known that Au particles provide high catalytic activity at temperatures above 180 °C.

- The effect of feed compositions can be further investigated such as effect of H2 or CO2 individually. Moreover, CH4 can be added to the feed gas to achieve a feed that simulates a typical fuel processor operation involving natural gas.

REFERENCES

1. Karakaya., M., "Experimental and Quantitative Analysis of Multiphase Catalytic Reactions under Microfluidic Flow Conditions and Geometries.", Ph.D. Thesis, Boğaziçi University, 2012.

2. Caglar., O. Y., "Parametric Study Of Water Gas Shift Reactiob Over Pt-Based Catalysts.", M.S. Thesis, Boğaziçi University, 2015.

3. Kim, K.-Y., J. Han, S. W. Nam, T.-H. Lim and H.-I. Lee, "Preferential oxidation of CO over CuO/CeO 2 and Pt-Co/Al 2 O 3 catalysts in micro-channel reactors", *Catalysis Today*, Vol. 131, No. 1, pp. 431–436, 2008.

4. Ratnasamy, C. and J. P. Wagner, "Water gas shift catalysis", *Catalysis Reviews*, Vol. 51, No. 3, pp. 325–440, 2009.

5. Smith, R., M. Loganathan, M. S. Shantha *et al.*, "A review of the water gas shift reaction kinetics", *International Journal of Chemical Reactor Engineering*, Vol. 8, No. 1, 2010.

6. Kolb, G., H. Pennemann and R. Zapf, "Water-gas shift reaction in micro-channels—Results from catalyst screening and optimisation", *Catalysis today*, Vol. 110, No. 1, pp. 121–131, 2005.

7. Baier, T. and G. Kolb, "Temperature control of the water gas shift reaction in microstructured reactors", *Chemical engineering science*, Vol. 62, No. 17, pp. 4602–4611, 2007.

8. Jeong, D.-W., W.-J. Jang, J.-O. Shim, W.-B. Han, H.-S. Roh, U. H. Jung and W. L. Yoon, "Low-temperature water–gas shift reaction over supported Cu catalysts", *Renewable Energy*, Vol. 65, pp. 102–107, 2014.

9. Wheeler, C., A. Jhalani, E. Klein, S. Tummala and L. Schmidt, "The water–gas-shift reaction at short contact times", *Journal of catalysis*, Vol. 223, No. 1, pp. 191–199, 2004.

10. Ehrfeld, W., V. Hessel and H. Lowe, *Microreactors: New Technology for Modern Chemistry*, Wiley, Weinheim, 2001.

11. Jähnisch, K., V. Hessel, H. Löwe and M. Baerns, "Chemistry in microstructured reactors", *Angewandte Chemie International Edition*, Vol. 43, No. 4, pp. 406–446, 2004.

12. Watts, P. and C. Wiles, "Recent advances in synthetic micro reaction technology", *Chemical communications*, , No. 5, pp. 443–467, 2007.

13. Tonkovich, A., D. Kuhlmann, A. Rogers, J. McDaniel, S. Fitzgerald, R. Arora and T. Yuschak, "Microchannel technology scale-up to commercial capacity", *Chemical Engineering Research and Design*, Vol. 83, No. 6, pp. 634–639, 2005.

14. Lin, K.-S., S. Chowdhury, H.-P. Yeh, W.-T. Hong and C.-T. Yeh, "Preparation and characterization of $CuO/ZnO–Al_2O_3$ catalyst washcoats with CeO_2 sols for autothermal reforming of methanol in a microreactor", *Catalysis today*, 2011.

15. Huang, C.-C., Y.-J. Huang, H.-S. Wang, F.-G. Tseng and Y.-C. Su, "A well-dispersed catalyst on porous silicon micro-reformer for enhancing adhesion in the catalyst-coating process", *international journal of hydrogen energy*, Vol. 39, No. 15, pp. 7753–7764, 2014.

16. De Farias, A. M. D., D. Nguyen-Thanh and M. A. Fraga, "Discussing the use of modified ceria as support for Pt catalysts on water–gas shift reaction", *Applied Catalysis B: Environmental*, Vol. 93, No. 3, pp. 250–258, 2010.

17. Chen, K.-Y., C.-C. Shen, C.-Y. Lee, S.-J. Lee, C.-H. Leu, J.-H. Wang and C.-T. Yeh, "Coating powdered copper catalyst with yttria sol", *Materials Chemistry and*

Physics, Vol. 128, No. 1, pp. 57–61, 2011.

18. Hilaire, S., X. Wang, T. Luo, R. Gorte and J. Wagner, "A comparative study of water-gas-shift reaction over ceria supported metallic catalysts", *Applied Catalysis A: General*, Vol. 215, No. 1, pp. 271–278, 2001.

19. Neuberg, S., S. Keller, M. O'Connell, J. Schürer, R. Thiele, R. Zapf, A. Ziogas and G. Kolb, "Effect of oxygen addition on the water–gas shift reaction over Pt/CeO 2 catalysts in microchannels–Results from catalyst testing and reactor performance in the kW scale", *International Journal of Hydrogen Energy*, Vol. 39, No. 31, pp. 18120–18127, 2014.

20. Germani, G. and Y. Schuurman, "Water-gas shift reaction kinetics over μ-structured Pt/CeO2/Al2O3 catalysts", *AIChE journal*, Vol. 52, No. 5, pp. 1806–1813, 2006.

21. Simsek, E., A. K. Avci and Z. I. Önsan, "Investigation of catalyst performance and microstructured reactor configuration for syngas production by methane steam reforming", *Catalysis today*, Vol. 178, No. 1, pp. 157–163, 2011.

APPENDIX A: MFC CALIBRATION CURVES

MFC calibration curves for all reactant and product gases are introduced in this section.

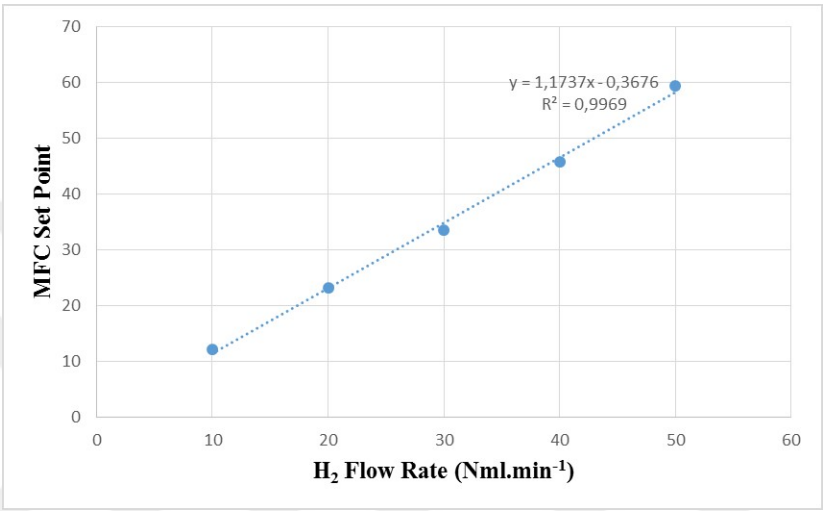

Figure A.1. MFC Calibration Curve of H_2.

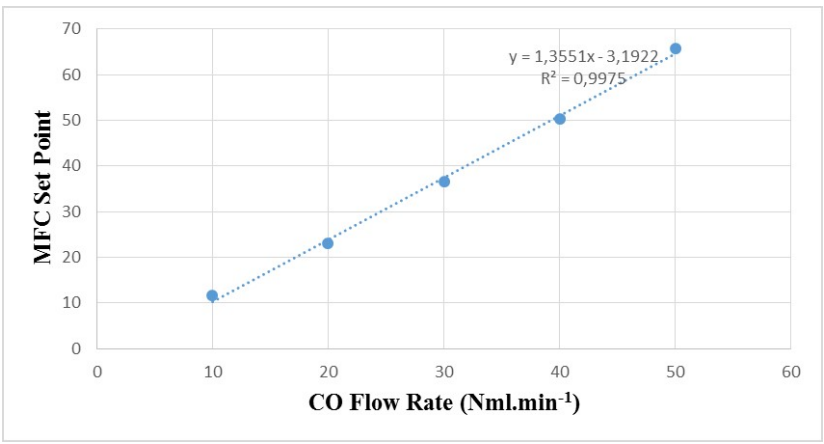

Figure A.2. MFC Calibration Curve of CO.

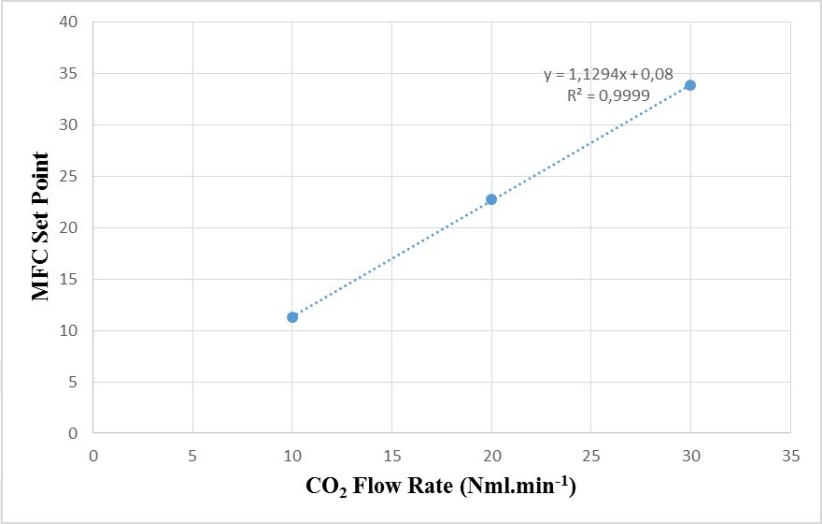

Figure A.3. MFC Calibration Curve of CO_2.

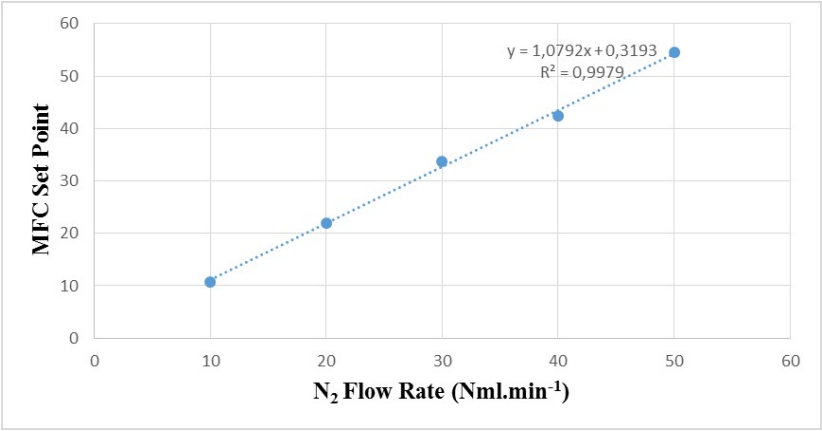

Figure A.4. MFC Calibration Curve of N_2.

APPENDIX B: GC CALIBRATION CURVES

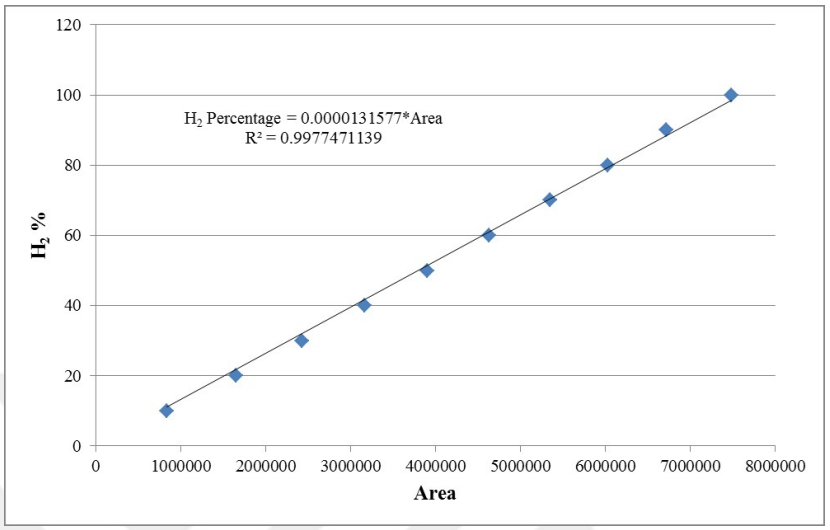

Figure B.1. GC Calibration Curve of H_2.

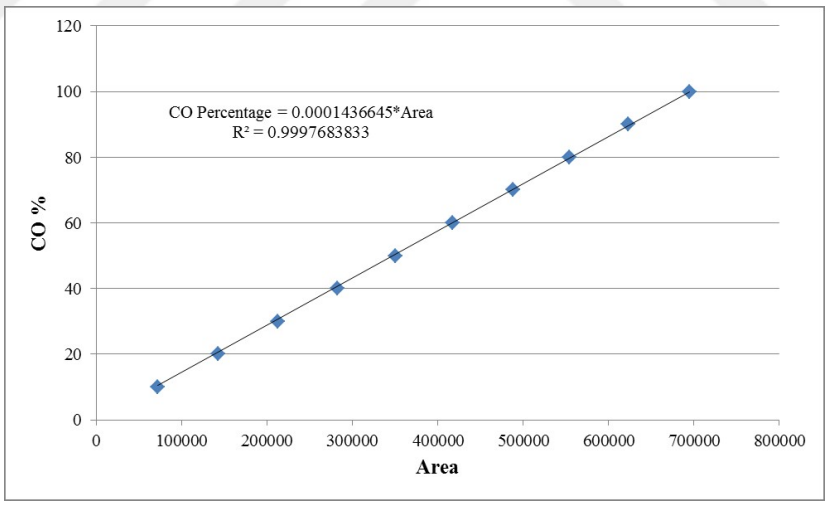

Figure B.2. GC Calibration Curve of CO.

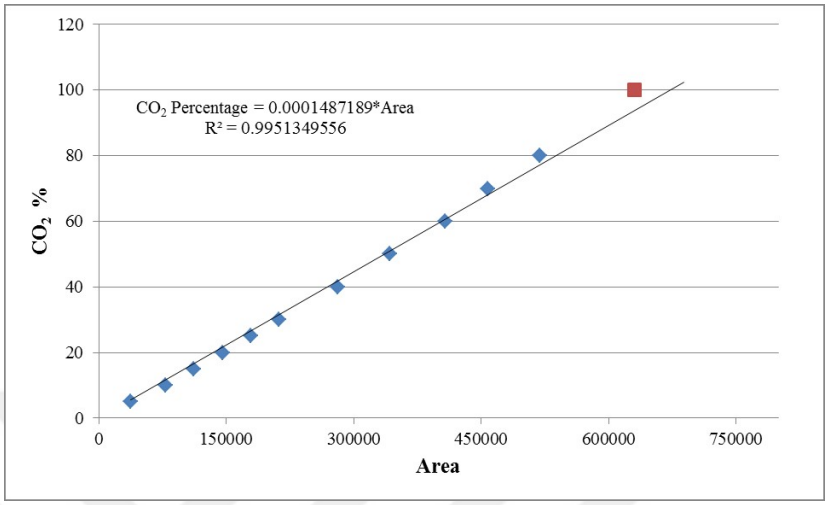

Figure B.3. GC Calibration Curve of CO_2.

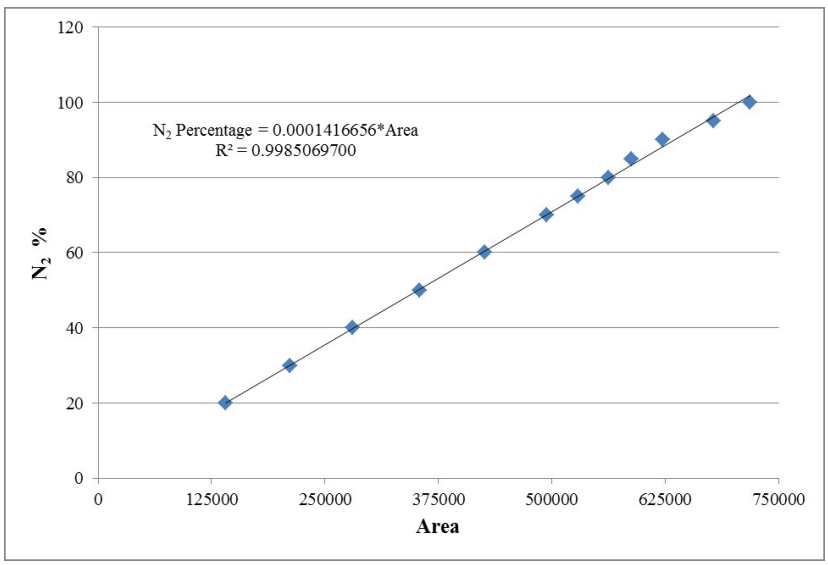

Figure B.4. GC Calibration Curve of N_2.